The Monte Carlo Method: Versatility Unbounded in a Dynamic Computing World
Chattanooga, Tennessee, April 17-21, 2005, on CD-ROM, American Nuclear Society, LaGrange Park, IL (2005)

A MONTE CARLO SOLUTION FOR EXTERNAL BEAM PHOTON RADIOTHERAPY VERIFICATION

P W Chin and D G Lewis
Department of Medical Physics, Velindre Cancer Centre
Cardiff, Wales, United Kingdom.
mary.chin@physics.org; dg.lewis@physics.org

J P Giddy
Welsh e-Science Centre, Cardiff University
Cardiff, Wales, United Kingdom.
j.p.giddy@wesc.ac.uk

ABSTRACT

In this work, Monte Carlo (MC) simulations provide an answer to the surging clinical need for verifying complex radiation treatments. As will be demonstrated, this solution attained accuracy (2% in dose prediction when compared to measured data, which is itself of comparable uncertainty) and versatility (over a wide range of clinical setups) known to be unachievable by other techniques. The solution is not impeded by long runtimes since it has been successfully implemented on the Grid. It can therefore be clinically productive. Implementation on the UK National Grid Service will be reported. This work also draws from MC simulation information beyond physical measurements, such as details about radiation interactions in a radiotherapy imager. Aided by this knowledge, we designed a simplified, substitute imager which reduces MC runtimes. It can also be useful for other dosimetric computation techniques where detailed modelling is unavailable. Additionally, we report a MC study on how a general assumption in non-MC techniques leads to inaccurate dose prediction.

Key Words: Radiotherapy, Verification, EPID, EGSnrc, BEAMnrc, Grid computing, Radiation detectors, Phantom design

1 INTRODUCTION

Advanced radiotherapy techniques involving conformal field shaping and/or intensity modulation require thorough verification. Treatment field configurations and dosimetric settings should be verified both before and during treatment. Pre-treatment verification ensures accurate dose calculation and accurate implementation of treatment planning system (TPS) generated parameters on the treatment machine. On-treatment verification ensures accurate dose delivery to the patient according to the treatment plan and clinical prescription.

Diodes and thermoluminescent dosimeters are conventionally used for treatment verification. However, since they are usually placed on the patient's skin surface, dose verification is usually limited to a number of superficial points. Portal films are also commonly used despite various deficiencies such as narrow latitude due to the film's characteristic curve, noise associated with film granularity, batch-to-batch inconsistencies, susceptibility to under- and over-exposures, and delay in film development. We report a treatment verification solution which combines the accuracy of Monte Carlo (MC) simulations with the technology of electronic portal imaging devices (EPIDs) – a facility for capturing 2D images by detecting radiation from the treatment beams transmitted through the patient [1].

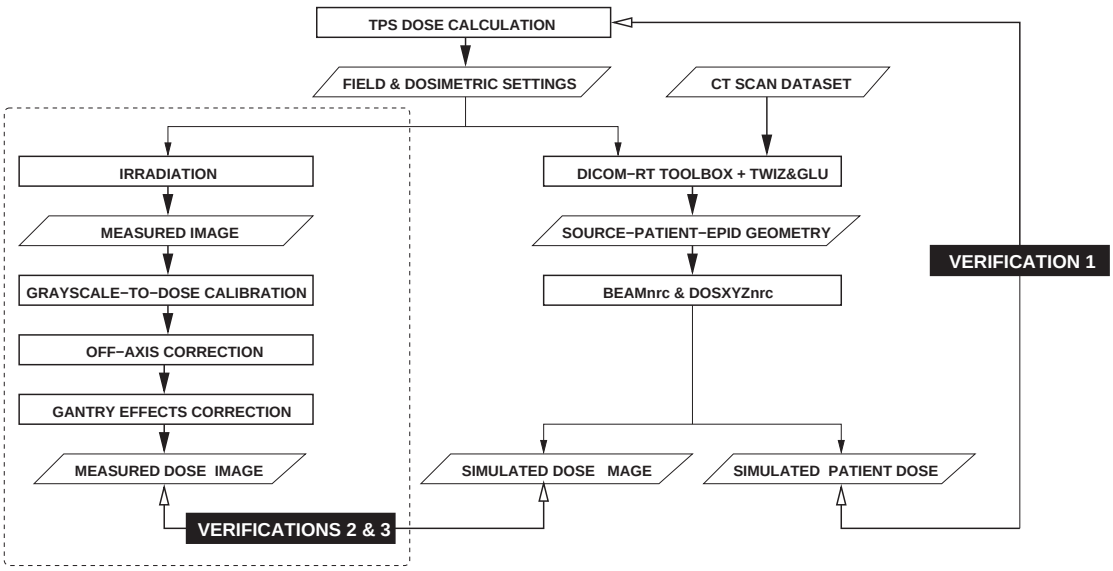

Figure 1: A MC dose calculation framework for verification at various stages: 1. verifying TPS dose calculation; 2. verifying implementation of TPS-generated parameters on treatment machine; 3. verifying patient dose delivery. Steps in the dashed box are repeated for subsequent treatment fractions.

2 MATERIALS & METHODS

Fig. 1 outlines the MC treatment verification framework. Measured images are calibrated for dose and corrected for off-axis variations [2]. Correction for gantry effects is needed for EPIDs of the scanning liquid ionisation chamber (SLIC) type, since its response varies with gantry angle [3]. An identical irradiation configuration would be MC-simulated with the EGSnrc-based BEAMnrc and DOSXYZnrc [4, 5, 6] using input files generated by the DICOM-RT toolbox [7] and TWIZ&GLU, which packages the CT phantom with an EPID according to the beam obliquity [8].

For each treatment case, MC simulation is performed once. From the same simulation, dose deposition can be obtained both in the patient and in the EPID (hence the predicted portal image). The former acts as an independent check to the TPS dose calculation. The latter forms the reference against which actual portal images, acquired pre-treatment and on-treatment, are verified.

The MC framework is based on complete modelling of the irradiation geometry: 1) the medical linear accelerator (linac) as the radiation source; 2) the CT scan data representing the inhomogeneous patient anatomy voxel-by-voxel; and 3) the EPID.

The following sections detail a study of radiation transport in the SLIC EPID, the design of a SLIC substitute, and a demonstration of MC portal dose prediction at various clinical setups. This is followed by a MC study on how a general assumption in non-MC techniques leads to inaccurate portal dose prediction for an amorphous silicon (a-Si) EPID. Finally, Grid-computing simulations on the UK National Grid Service (NGS) will be described.

2.1 Radiation Transport Studies

A dosimetrically working model of the SLIC EPID has been previously reported [2]. The full model contains 15 layers of different materials according to manufacturer's specifications (Fig. 2). To facilitate our understanding of radiation transport in the SLIC, we ran EGSnrc codes to tally the interaction type, energy deposition and backscatter contribution in each layer. The EPID was irradiated by a 6 MV, 10 cm square beam.

2.2 Design of a SLIC Substitute

The detailed layered models entail frequent boundary crossing during MC simulations (causing long runtimes) and cannot be readily implemented for non-MC calculations (e.g. conventional TPSs, convolution/superposition techniques.) A simplified model could therefore be useful as a SLIC substitute for dosimetric computation. Aided by results from the above radiation transport studies, we designed a 4-layer SLIC substitute comprising:

1. the top cover, of a media composed of elements from the polystyrene, air, rohacell (foam) and two FR4 (printed circuit board) layers of the original model. By specifying the summed proportion-by-weight of each element, cross section data for the media were generated using preprocessor PEGS4 [9]. To maintain the beam divergence incident on the active detection layer, thickness of the top cover was kept at the total thickness of the layers it replaced. The density was calculated so that the total weight remained unchanged.
2. the buildup or photon-to-electron converter (plastoferrite), is kept but relocated immediately upstream to the active detection layer.
3. the active detection layer (isooctane), is left unchanged.
4. the back cover, is reduced to a single layer of FR4.

All copper layers (each 1.6 μm-thick) were not included. The SLIC substitute was tested against the full model by comparing portal dose profiles, along the patient right-left direction, over a range of irradiation setups: 2 cm, 10 cm, 20 cm square beams, and a 20 cm square beam attenuated by a 20 cm $\times$ 20 cm $\times$ 20 cm water slab positioned at source-surface distance 114 cm, which resulted in the minimum phantom-to-EPID air gap distance for a source-detector distance of 140 cm. The short air gap distance was to provide a high scatter condition.

2.3 Demonstrations: Monte Carlo Portal Dosimetry

The accuracy of MC portal dose simulation for the SLIC was tested over a wide range of clinical setups: field sizes from 5 cm $\times$ 5 cm to 25 cm $\times$ 25 cm; phantom-to-EPID air gap distance from 4 cm to 38 cm; presence of an inhomogeneous phantom; and gantry angles at varying tilts from the vertical. Used for the tests were a homogeneous phantom (20 cm $\times$ 20 cm $\times$ 20 cm perspex) and an inhomogeneous phantom (20 cm $\times$ 20 cm $\times$ 20 cm perspex with a 4 cm-thick, 5 cm $\times$ 5 cm air cavity at the centre). Profiles extracted from measured and simulated dose images, after applying the necessary calibration and corrections (Fig. 1), were compared.

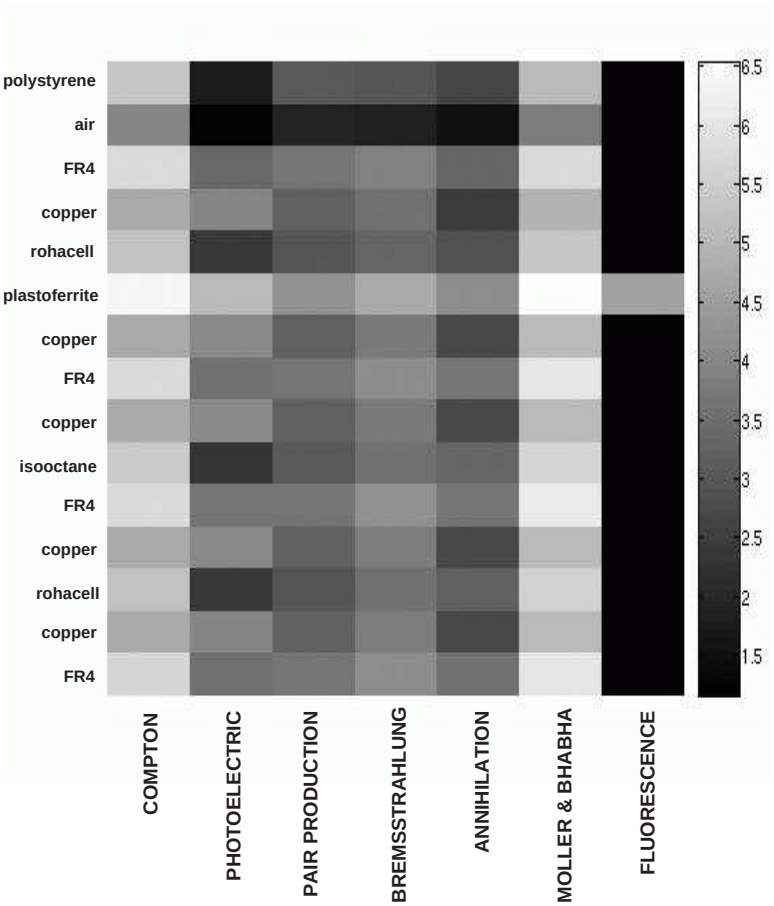

Figure 2: Count of each interaction type in each layer of the SLIC. Grayscale is in $\log_{10}$. Thicknesses do not reflect true layer thicknesses.

2.4 Comparison with Other Techniques

Non-MC portal dose prediction techniques typically assume the EPID to be water-equivalent (e.g. [10] and [11].) We investigated how far this assumption is true by simulating a water slab and extracting dose profiles at the depth of maximum dose under 4 irradiation conditions, similar to those in Section 2.2. These profiles were compared against profiles from a complete a-Si model [12].

2.5 Simulations on the UK National Grid Service

Serial computation of millions of histories requires long runtimes, which is clinically impractical. However, the lack of dependencies between individual particle histories makes it simple to distribute history ranges to different processors to shorten the overall runtime. We have previously Grid-enabled EGSnrc, BEAMnrc and DOSXYZnrc simulations [13]. Recently, we gained access to the UK National Grid Service (NGS), the core production-level grid created under the UK e-Science program. It uses grid middleware (the Globus Toolkit) to provide secure remote access to a collection of hardware, software and support resources available to the UK

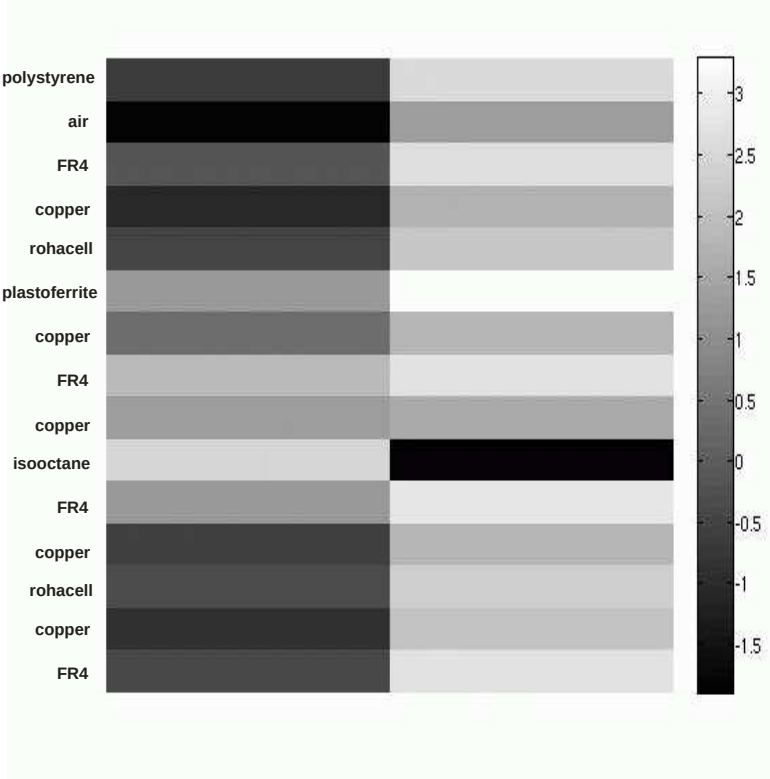

Figure 3: Energy deposition in each layer, by particles which deposited energy in the isooctane layer (left), and those which did not deposit energy in the isooctane layer (right). Grayscale is in $\log_{10}$. Thicknesses do not reflect true layer thicknesses.

academic community. Globus also hides some system heterogeneity, such as the use of different batch queue systems such as Condor or PBSPro to queue and start computations [14]. Authentication is performed using digital certificates issued by the UK e-Science Certificate Authority.

Simulations in Section 2.3 was accomplished using the NGS. Nimrod/G was used as a high-level tool to create and monitor the individual jobs, and as a broker to choose on which resources jobs should run [15]. The gain in runtime will be reported.

3 RESULTS & DISCUSSION

3.1 Radiation Transport Studies

Fig. 2 shows the count for each interaction type. 40% of the events took place in the plastoferrite layer, 10% in each FR4 layer and 1% in each copper layer (1.6 μm-thick). The plastoferrite layer exhibited its distinctive role as buildup and converter. It contains strontium, which has an absorption edge at 16.1 keV. This explains the fluorescence. No other element in the SLIC model has an absorption edge above 10 keV, below which electron interactions were not

simulated explicitly. The isooctane (2,2,4 trimethylpentane) layer is the active detection area of the SLIC where signal is readout for image formation. In this layer, 33% were Compton events, while photoelectric events were 3 orders of magnitude lower.

Event counts, however, may not reflect the amount of energy absorbed. Fig. 3 shows the energy deposition in each layer, by particles which deposited energy in the isooctane layer (left), and those which did not (right). The latter indicates redundancy in computation time since these were the events which did not contribute to the detector signal. As expected, energy deposition was highest in the isooctane layer (66% of the total). Backscatter contributed to 15% of the total energy deposited in the isooctane layer. From backscatter particles which contributed to detector signal, 92% energy deposition was in the FR4 layer immediately downstream from the active detection layer.

3.2 Design of a SLIC Substitute

Fig. 4 compares portal dose profiles from the SLIC substitute and that from the complete model. (In this paper, where both sides of the profile are symmetrical, values at symmetrical points have been averaged and plotted as a single point.) Except for a few outliers due to statistical noise, agreement is under 1% of the central axis dose for all 4 irradiation configurations tested. Agreement is excellent since the formulation was not subjected to the many constraints and approximations in physical phantom fabrication [16]. The SLIC substitute halved the MC runtime for portal dose prediction of unattenuated fields.

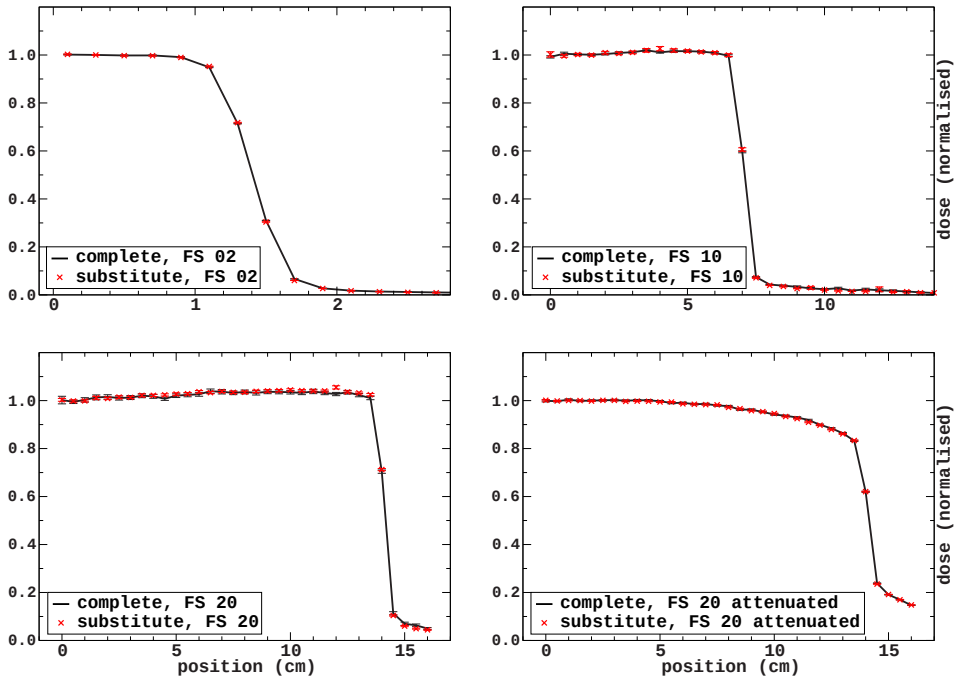

Figure 4: Comparison between the SLIC substitute and the complete SLIC model: portal dose profiles.

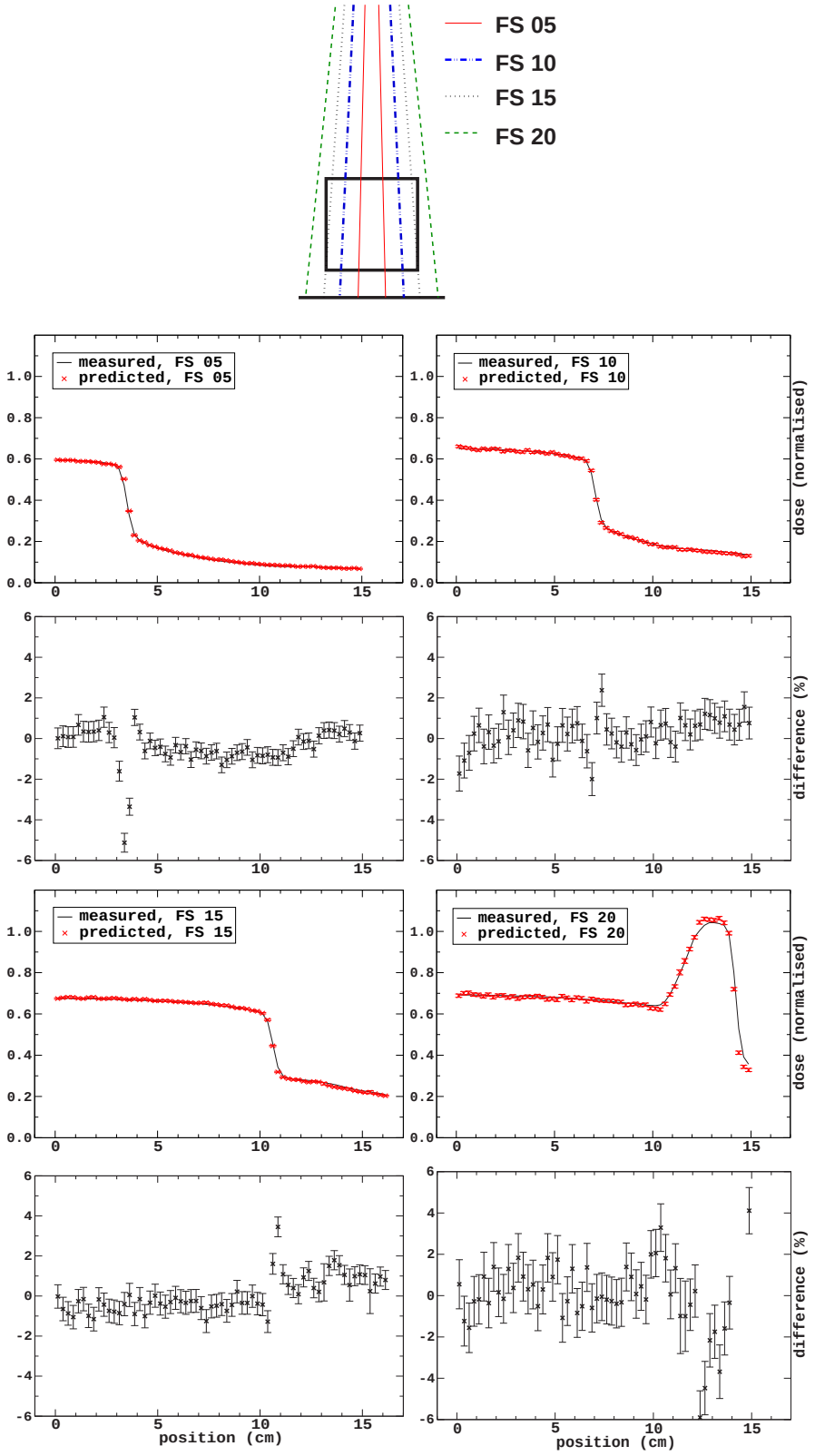

Figure 5: Irradiation of a homogeneous phantom at 5 cm, 15 cm and 20 cm square field sizes: the beam-phantom-EPID setup, the predicted and measured portal dose profiles, and the corresponding differences.

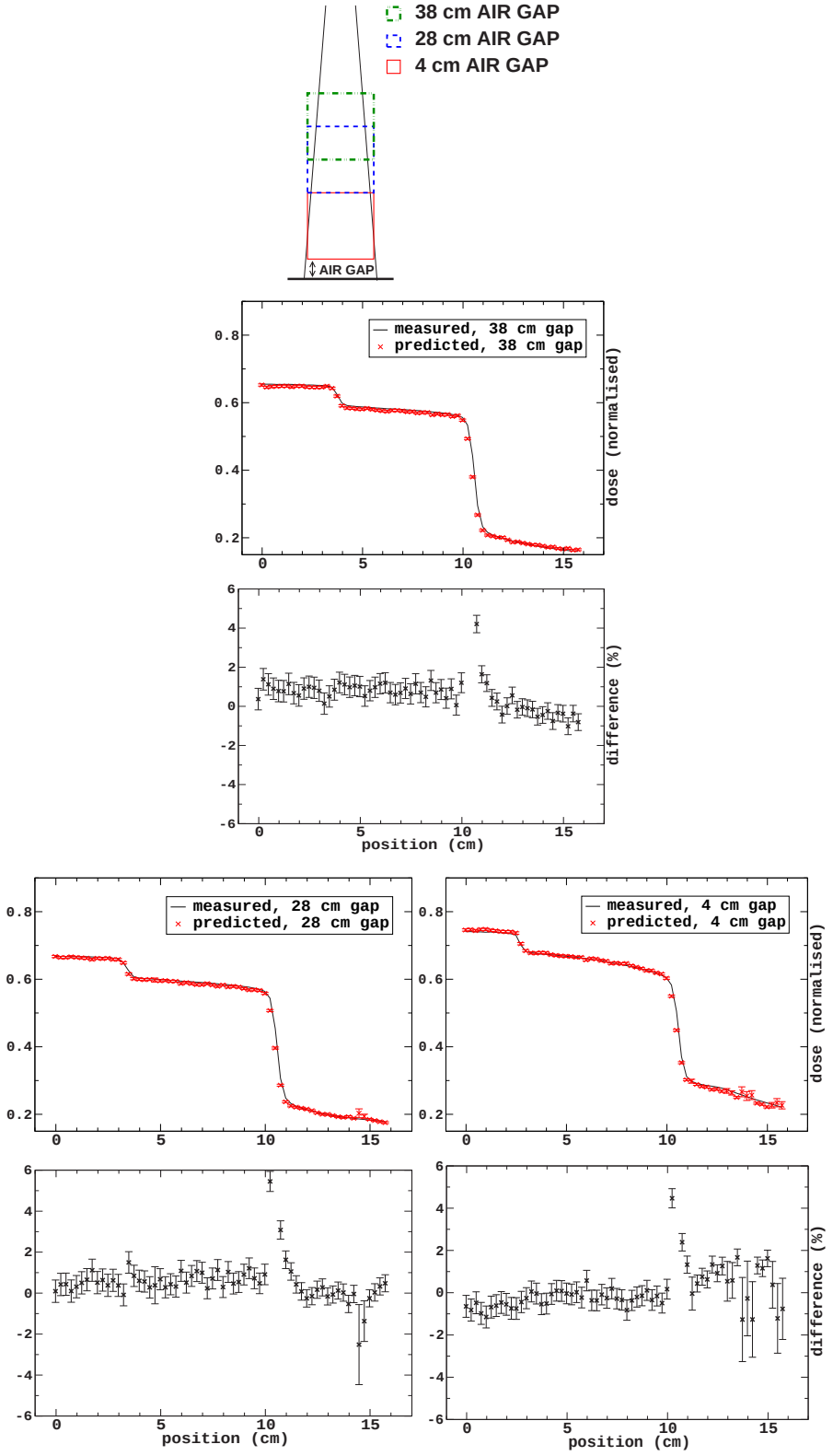

Figure 6: Irradiation of a inhomogeneous phantom at air gap distances 38 cm, 28 cm and 4 cm: the beam-phantom-EPID setup, the predicted and measured portal dose profiles, and the corresponding differences.

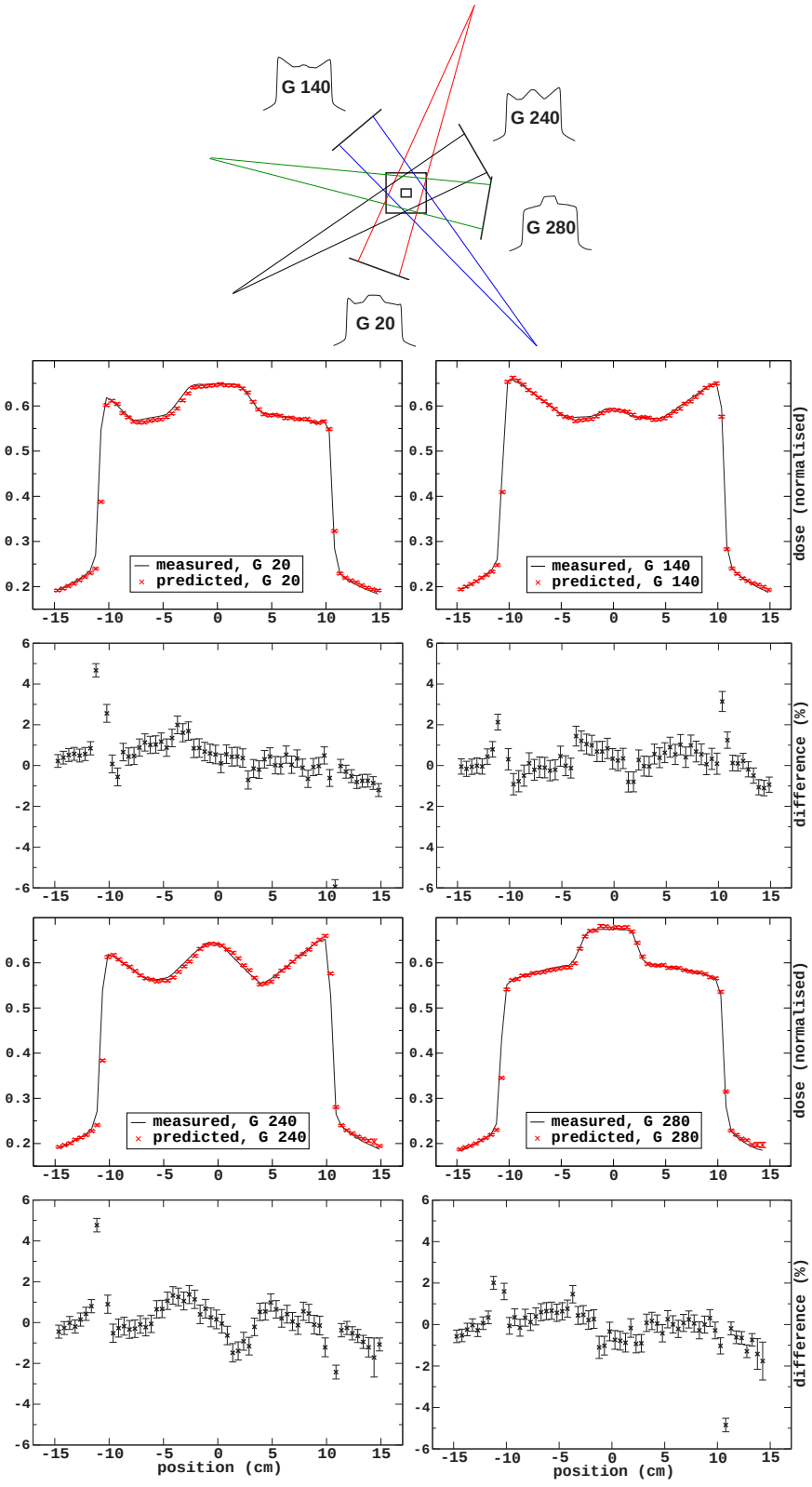

Figure 7: Isocentric irradiation of an inhomogeneous phantom at gantry angles 20°, 140°, 240° and 280°: the beam-phantom-EPID setup, the predicted and measured portal dose profiles, and the corresponding differences.

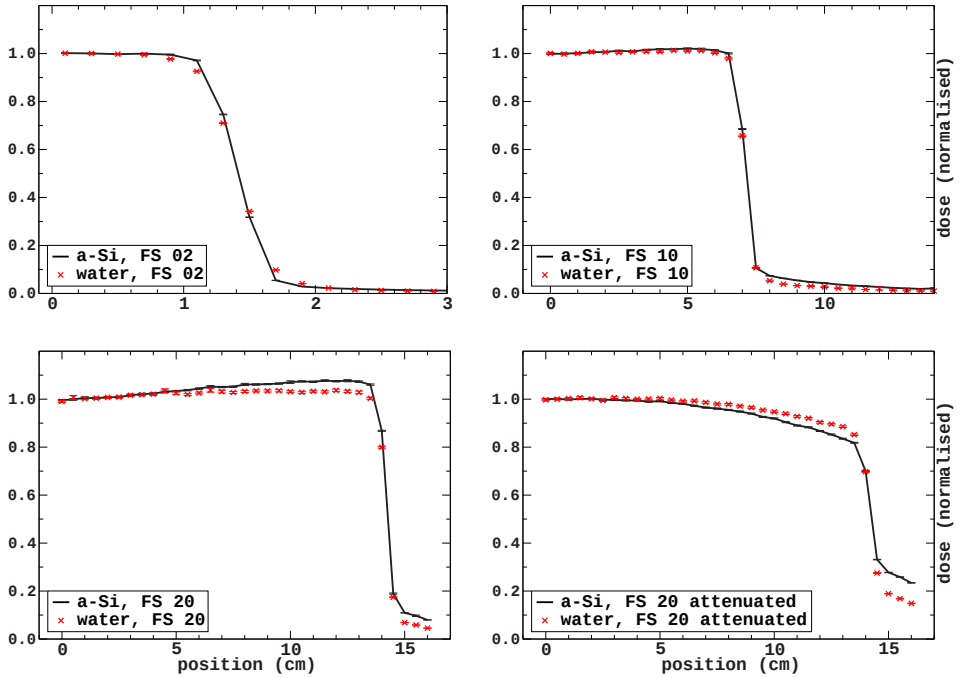

Figure 8: Comparison between the water slab and the complete a-Si model: portal dose profiles.

3.3 Demonstrations: Monte Carlo Portal Dosimetry

Agreement between simulated and measured portal dose profiles was generally within 2% of the central axis dose (Fig. 5, 6 and 7), except in regions of high dose gradient which are particularly susceptible to positional uncertainties of the diode and linac jaws during measurements. No field size dependence was observed. There was no loss of accuracy 1) in high scatter conditions when the phantom-to-EPID separation was only 4 cm; 2) with the presence of a 20 cm cubic perspex phantom, even when a 4 cm-thick, 5 cm $\times$ 5 cm air cavity was introduced at its centre; 3) when the gantry was rotated for delivery of oblique beams; and 4) in the absence of additional buildup on the EPID. Such inclusive versatility is known to be unachievable in non-MC portal dosimetry [10, 17, 18].

3.4 Comparison with Other Techniques

Fig. 8 compares portal dose profiles from the water slab model with that from the complete a-Si model. Deviations up to 10% of the central axis dose were found. We believe this explains the discrepancies reported in water-based portal dosimetry pursued elsewhere.

3.5 Simulations on the UK National Grid Service

For the investigation on variable gantry angles described in Section 2.3, the geometry contained 613,125 voxels. Incident beam was a 15 cm square field. Tally voxels, each of 0.08 cm $\times$ 0.5 cm $\times$ 3.0 cm, achieved 1% uncertainty in the penumbra and 0.4% in the beam. This

problem would have taken 6 days on a single 2.66 GHz Intel Pentium 4 processor.

The NGS provides access to 168 dedicated dual 3.06 GHz Intel Xeon nodes (336 processors in total) spread over four UK sites. Using the NGS, and in competition with other users' computations, the DOSXYZnrc simulation took less than 3 hours to complete. This is a 50-fold increase in the speed of computation, and brings the runtime much closer to an acceptable time frame for clinical operation.

The use of the NGS allowed us to achieve this speed-up without purchasing additional resources, and the time and costs of installing and maintaining a computational cluster ourselves. In a clinical setting, the capital and labour costs of obtaining this computational power and the expertise to run it are usually unavailable.

4 CONCLUSIONS

A versatile MC solution for external beam photon radiotherapy verification has been validated under a wide range of clinical setups. Off-axis agreement with portal dose profiles was within 2% of the central axis value. This combined versatility and accuracy is known to be not readily achievable by other techniques. The solution is not impeded by long runtimes since it has been successfully implemented on the Grid, which potentially harnesses resources around the world.

A SLIC substitute for dosimetric computation has been found. Under the irradiation conditions tested, dose profiles were within 1% agreement to that of the complete model.

The assumption of water-equivalence of EPIDs, intrinsic in many non-MC portal dosimetry techniques, was found to produce off-axis deviations in dose profiles up to 10% for the a-Si EPID. Our findings underscore the role of, and the need for, MC radiation transport in radiotherapy dosimetric calculation.

5 ACKNOWLEDGEMENTS

P W Chin is grateful to Cancer Research Wales and Yr Ysgol Uwchradd Tregaron for PhD funding.

6 REFERENCES

1. L. E. Antonuk, "Electronic portal imaging devices: a review and historical perspective of contemporary technologies and research," *Phys Med Biol*, **47**, pp. R31-65 (2002).
2. E. Spezi and D. G. Lewis, "Full forward Monte Carlo calculation of portal dose from MLC collimated treatment beams," *Phys Med Biol*, **47**, pp. 377-90 (2002).
3. P. W. Chin, D. G. Lewis and E. Spezi, "Correction for dose-response variations in a scanning liquid ion chamber EPID as a function of linac gantry angle, " *Phys Med Biol*, **49**, pp. N93-103 (2004).
4. I. Kawrakow, "Accurate condensed history Monte Carlo simulation of electron transport. I. EGSnrc, the new EGS4 version," *Med Phys*, **27**, pp. 485-98 (2000).

5. D. W. O. Rogers, C-M Ma, B. Walters, G. X. Ding, D. Sheikh-Bagheri and G. Zhang, “BEAMnrc Users Manual, NRCC Report PIRS-0509A,” NRCC, Ottawa, Canada (2001).
6. B. R. B. Walters and D. W. O. Rogers, “DOSXYZnrc Users Manual, NRCC Report PIRS-794,” NRCC, Ottawa, Canada (2002).
7. E. Spezi, D. G. Lewis and C. W. Smith, “A DICOM-RT-based toolbox for the evaluation and verification of radiotherapy plans,” *Phys Med Biol*, **47**, pp. 4223-32 (2002).
8. P. W. Chin, E. Spezi and D. G. Lewis, “Monte Carlo simulation of portal dosimetry on a rectilinear voxel geometry: a variable gantry angle solution,” *Phys Med Biol*, **48**, pp. N231-8 (2003).
9. I. Kawrakow and D. W. O. Rogers, “The EGSnrc Code System: Monte Carlo Simulation of Electron and Photon Transport, NRCC Report PIRS-701,” NRCC, Ottawa, Canada (2002).
10. R. Boellaard, M. van Herk and B. J. Mijnheer, “The dose response relationship of a liquid-filled electronic portal imaging device,” *Med Phys*, **23**, pp. 1601-11 (1996).
11. E. E. Grein, R. Lee and K. Luchka, “An investigation of a new amorphous silicon electronic portal imaging device for transit dosimetry.,” *Med Phys*, **29**, pp. 2262-8 (2002).
12. J. V. Siebers, J. O. Kim, L. Ko, P. J. Keall and R. Mohan, “Monte Carlo computation of dosimetric amorphous silicon electronic portal images,” *Med Phys*, **31**, pp. 2135-46 (2004).
13. P. W. Chin, D. G. Lewis and J. P. Giddy, “Implementation of BEAMnrc Monte Carlo simulations on the GRID,” *Proc. 14th Int. Conf on the Use of Computers in Radiation Therapy,* Seoul, May 2004, pp. 524-6 (2004).
14. I. Foster and C. Kesselman, “The Grid 2: Blueprint for a New Computing Infrastructure,” Morgan Kaufmann, San Francisco, USA (2004).
15. D. Abramson, J. Giddy, L. Kotler, “High-performance parametric modeling with Nimrod/G. Killer Application for the global grid?” *International Parallel and Distributed Computing Symposium* Cancun, Mexico, May 2000, pp 520-8 (2000).
16. “Tissue Substitutes in Radiation Dosimetry and Measurement, ICRU Report 44,” ICRU, Bethesda, USA (1988).
17. S. C. Vieira, M. L. Dirkx, B. J. Heijmen, H. C. de Boer, “SIFT: a method to verify the IMRT fluence delivered during patient treatment using an electronic portal imaging device,” *Int J Radiat Oncol Biol Phys*, **60**, pp.981-93 (2004).
18. A. van Esch, T. Depuydt and D. P. Huyskens, “The use of an aSi-based EPID for routine absolute dosimetric pre-treatment verification of dynamic IMRT fields,” *Radiother Oncol*, **71**, pp. 223-34 (2004).